

## EVALUATIONS OF EXISTING METHODS

# Bed-level tools for monitoring erosion and accretion patterns: Flume validation and field testing

Lucía Rodríguez-Arias <sup>1,2,\*</sup>, Inés Mazarrasa,<sup>3</sup> Beatriz Marin-Diaz,<sup>4</sup> Teresa Alcoverro,<sup>1</sup> Barbara Ondiviela,<sup>3</sup> Jordi F. Pagès,<sup>1</sup> Eduardo Infantes<sup>5,6</sup>

<sup>1</sup>Centre d'Estudis Avançats de Blanes (CEAB-CSIC), Catalonia, Spain; <sup>2</sup>Department of Evolutionary Biology, Ecology and Environmental Sciences, University of Barcelona, Catalonia, Spain; <sup>3</sup>IHCantabria – Instituto de Hidráulica Ambiental de la Universidad de Cantabria, Santander, Spain; <sup>4</sup>Department of Marine Ecology, Mediterranean Institute for Advanced Studies (IMEDEA, CSIC-UIB), Esporles, Spain; <sup>5</sup>Department of Biological and Environmental Sciences, Kristineberg, University of Gothenburg, Fiskebäckskil, Sweden; <sup>6</sup>Department of Biology, Campus Tafira, University of Las Palmas de Gran Canaria, Las Palmas, Canary Islands, Spain

### Abstract

Monitoring short-term changes in surface sediment elevation is fundamental to understanding erosion, transport, and deposition dynamics in shallow coastal environments. However, commonly used field approaches, such as horizontal markers, sediment erosion tables, subsurface sediment plates, or erosion pins, are not always cross-validated under both controlled and field conditions, limiting confidence in their comparative performance. This study experimentally evaluates the performance and potential biases of two widely used and cost-effective bed-level monitoring tools: (1) subsurface sedimentation plates (without string, with string, and with string and buoy) and (2) sedimentation bars. Methods were evaluated under controlled conditions in a hydraulic flume using non-cohesive sandy sediment. Plates and bars were subjected to unidirectional and oscillatory flow regimes at two velocity levels (11 and 23 cm s<sup>-1</sup>) to compare their erosion responses and assess the hydrodynamic interference generated by their structural components, quantified through Reynolds numbers. A complementary field deployment was conducted over 1 year in a *Zostera marina* meadow in the Bay of Santander estuary (Spain). Across flume flow regimes and field habitats, bed-level change estimates were comparable among methods, with no detectable differences within the resolution of the experimental design (minimum detectable difference ≈ 1.9 mm for current-driven and 2.5 mm for wave-driven conditions). Although the buoy produced localized turbulence, the resulting shear stress was likely below critical erosion thresholds. Together, the results support the use of sedimentation plates (with or without string or buoy) and bars as practical cost-effective tools for monitoring short-term bed-level change in shallow, non-cohesive sandy and vegetated environments.

Short-term bed-level change in shallow coastal waters results from complex interactions among hydrodynamics, topography and roughness elements, such as bedforms or vegetation (Nepf 2012; Yang and Nepf 2019). Sediment erosion

from the surface layer can result either from horizontal bedload transport or vertical suspended load (Einstein et al. 1940; Soulsby and Damgaard 2005). Bedload transport involves the horizontal movement of particles along the seabed, contributing to changes in surface elevation (Soulsby and Damgaard 2005). In contrast, resuspension occurs when sediment particles are lifted vertically into the water column, increasing turbidity and reducing light availability (Brown et al. 1995; Einstein et al. 1940). Understanding sediment transport in coastal habitats has become crucial for ecosystem resilience (Temmerman et al. 2013), considering that some

\*Correspondence: [lucia.rodriquez@ceab.csic.es](mailto:lucia.rodriquez@ceab.csic.es)

This is an open access article under the terms of the [Creative Commons Attribution](https://creativecommons.org/licenses/by/4.0/) License, which permits use, distribution and reproduction in any medium, provided the original work is properly cited.

Associate editor: Xiao Hua Wang

coastal landscapes are very sensitive to erosion and burial (Blum and Roberts 2009; Cabaço et al. 2008; Gera et al. 2014; McLeod et al. 2011). Although several methods exist to monitor short-term bed-level change, they are rarely cross-validated under both controlled and field conditions. As a result, no broadly applicable protocols exist and data comparability across habitats remains limited.

In many coastal zones, currents and waves are the primary drivers of sediment dynamics, causing sufficient shear stress to erode and transport particulate material (Butman et al. 1979; Nittrouer and Wright 1994; Soulsby et al. 1993). Coastal morphology co-evolves over both short and long timescales, but changes are not always progressive (Wright and Thom 2023). The magnitude and frequency of these hydrodynamic drivers can drive rapid coastal morphological adjustments, especially during storms or high-energy events (Sclavo et al. 2013; Woodroffe and Murray-Wallace 2012). At the same time, the inherent dynamism and vulnerability of coastal ecosystems render them particularly sensitive to small changes in elevation (Russell et al. 2022). To effectively predict and manage coastal morphological changes, in situ short-term observations are required to capture the spatial and temporal variability governing the erosion and deposition of surface sediment (Larson et al. 1997). This is particularly relevant in seagrass habitats, where oscillatory flow can strongly influence both bed-load transport and sediment resuspension (Marin-Diaz et al. 2020).

Several methods have been developed to quantify sediment elevation changes in intertidal and subtidal environments, but each approach has specific advantages and limitations (see the full reviews by Nolte et al. 2013; Thomas and Ridd 2004). For example, erosion pins are inexpensive and easy to deploy but may distort local hydrodynamics and mask the magnitude of overall soil movement (Haigh 1977; Kearney et al. 2018). Horizon makers provide high-resolution measurements and can be combined with surface elevation table-marker horizon (SET-MH); however, feldspar marker-horizons are vulnerable to subsidence and erosion by physical processes, and may wash away in submerged environments (Potouroglou et al. 2017; van Wijnen and Bakker 2001). Surface elevation tables and rod surface-elevation table (RSETs) allow precise vertical change measurements but are unsuitable for high-energy environments (Boumans and Day 1993; Cahoon et al. 2002a, 2002b; Van Duin et al. 1997), while sedimentation-erosion bars offer broader spatial coverage but with lower accuracy compared to SETs (Nolte et al. 2013), and neither can quantify erosion. Another example is the subsurface sediment plates, which are simple and low-cost and provide direct evidence of accretion or erosion over time and space (Marin-Diaz et al. 2025; Lewis and McGlathery 2023; Swales and Lovelock 2020). Emerging technologies such as the differential Global Navigation Satellite System (GNSS) and Unmanned Aerial Vehicle (UAV)-based photogrammetry techniques have enabled high-resolution, three-dimensional characterization

of sediment surfaces and volumetric sediment dynamics. However, their application remains limited by cost, specialized equipment and personnel, and logistical complexity, particularly for optical constraints in shallow (or vegetated) aquatic environments (Beca-Carretero et al. 2020; Gray et al. 2022; Kaufman and Bell 2022; Veetil et al. 2020).

Given the diversity of available approaches, empirical cross-method comparisons and standardized protocols are fundamental to reducing uncertainty. Although comparative assessments do exist, they are typically limited in scope or context. This is particularly important because no single method is universally applicable, and site-specific or combined approaches may be needed to generate reliable datasets. Consequently, the comparability of measurements obtained with different bed-level and low-cost tools, as well as the potential influence of deployment-related structural elements (e.g., strings, buoys, or exposed rods) on measurement outcomes remains insufficiently constrained.

Here, we evaluate the performance and potential biases of two commonly used and cost-effective field methods, subsurface plates and sedimentation erosion bars, for measuring short-term sediment elevation changes in shallow coastal habitats. Specifically, we tested (1) Do these methods yield comparable erosion and deposition estimates under controlled hydrodynamic conditions? (2) Are any of them prone to flow-induced bias or turbulence artifacts? (3) Do field measurements across vegetated and unvegetated areas confirm method consistency? To answer these questions, the methods were tested using a hydraulic flume under controlled surface-sediment erosion conditions across a range of both current and wave orbital velocities. Their performance was further verified under natural conditions through a one-year deployment in a *Zostera marina* seagrass meadow. By testing their reliability and comparability, we provide practical guidance for selecting methods according to site-specific conditions, supporting the use of simple, robust, and comparable tools for monitoring sedimentation dynamics in coastal (vegetated and unvegetated) aquatic ecosystems.

## Materials and procedure

### Experimental methods to test and sediment preparation

We tested two methods (sedimentation plates and sedimentation bars, commonly used in shallow soft-bottom coastal studies) to measure sediment surface changes under controlled and natural conditions (i.e., flume and field experiment, respectively). The plate method was tested in three variants: plate without string, with string, and with string and buoy to evaluate whether the retrieval aids (i.e., string and buoy) had additional effects on the sediment surface change. The string attached to the plate facilitates retrieval, and the buoy adds an extra element marker that maintains the string accessible by preventing its burial. In total, the four experimental setups included (1) plate, a horizontal methacrylate plate of

10 × 10 cm and 1 cm width (only deployed in the flume experiment, not included in the field experiment, to avoid retrieval problems); (2) plate + string, a horizontal methacrylate plate of 10 × 10 cm and 1 cm width with an added string (ø 4 mm) attached to the middle of the plate; (3) plate + string + buoy, a methacrylate plate of 10 × 10 cm and 1 cm width with a string and a 4-cm diameter fishing buoy attached to the string; and (4) steel rebar, a 1 cm diameter and 0.15 m long in the flume, and a bamboo bar, 0.3 m long in the field experiment (Fig. 1a; Supporting Information Fig. S1).

### Flume setup and flow regime

The performance and potential bias of the different bed-level measurement methods were evaluated under controlled flume conditions by testing the influence of hydrodynamic forcing, specifically unidirectional (i.e., current) and oscillatory (i.e., waves) flows, on surface sediment erosion. This study was conducted in a hydraulic flume at the Kristineberg Marine Research Station. The flume measured 8 m in length, 0.5 m in width, and 0.5 m in depth, and included a 2 m long test section consisting of a 0.35 × 0.35 × 0.15 m (length × width × height) cavity containing the substrate to install the plates and bars. The flume was able to simulate both unidirectional and oscillatory flow, generating realistic conditions representative of the field (Infantes et al. 2021; Fig. 1b,c; Supporting Information Fig. S2).

Unidirectional flow velocities were generated by a motor-run propeller at the end of the flume, controlled by an adjustable speed drive (Dayton Electronic, model 6K119), regulating the revolution per minute. In the unidirectional flow setup, water was recirculated through a pipe installed at the base of the flume, where the propeller was also situated (Infantes et al. 2021). Oscillatory flow velocities were generated by a pneumatic piston (Festo®) linked to a plexiglas paddle mounted on a rolling cart. The orbital magnitude, amplitude, and frequency of the generated waves were controlled by a computer program, allowing for adjustments in the distance and speed of the piston's stroke. To prevent wave reflections at the end of the flume, a PVC wave absorber covered by synthetic fibers and inclined at 15° was installed at the end of the flume (Infantes et al. 2021). The flume was directly filled with seawater from Gullmars Fjord, with a salinity of 27.65‰ and a temperature of 15°C ± 1°C. Therefore, the water density and viscosity were  $\rho_w = 1020.36 \text{ kg m}^{-3}$  and  $\mu_w = 1.206 \times 10^{-3} \text{ Pa s}^{-1}$ , respectively. The flume was filled to a standardized water column height of 0.15 m and maintained throughout all run-ups and measurements.

The flow of each regime was measured using an Acoustic Doppler Velocimeter (Nortek, Vectrino) mounted on a three-dimensional positioning system. The positioning system was configured with  $x$  defined as the position along the flume channel axis,  $y$  as the distance across the flume, and  $z$  as the vertical dimension. The Acoustic Doppler Velocimeter was placed in the center of the test section and measured 1–2 cm below the water surface. The sampling frequency was 25 Hz

for 3 min, resulting in 4500 measurements. For unidirectional flow, flow velocity was calculated as the average velocity, and for oscillatory flow, the mean of flow orbital velocities ( $U_{\text{rms}}$ ,  $\text{cm s}^{-1}$ , Eq. 1) was calculated as the mean fluctuating velocity over the oscillatory cycle.

$$U_{\text{rms}} = \sqrt{\frac{1}{n} \sum_{i=1}^n u_i^2} \quad (1)$$

where  $u$  is the horizontal flow velocity at  $n$  measurement points.

To characterize the flow regime and to contextualize the experimental conditions within the range of shallow-water flows, the Froude number (Fr) was calculated for the flume experiments (Chanson 2004; Soulsby 1997) (Eq. 2):

$$\text{Fr} = \frac{U}{\sqrt{gh}} \quad (2)$$

where  $U$  corresponds to mean flow velocity in the flume ( $U = 0\text{--}23 \text{ cm s}^{-1}$ ),  $g$  is the gravity ( $g = 9.81 \text{ m s}^{-2}$ ), and  $h$  is the water column depth ( $h = 15 \text{ cm}$ ). Flow conditions in the flume remained subcritical ( $\text{Fr} < 1$ ) for all tested current and wave velocities, with Froude numbers ranging from 0.09 to 0.18 for currents and from 0.09 to 0.19 for waves, consistent with shallow coastal environments where currents are slower than gravity-wave propagation.

### Hydrodynamic treatment

The sediment substrate was collected from Gullmars Fjord on the Swedish Skagerrak coast (58°14'N, 11°26'E) by snorkeling. The sediment consisted solely of non-cohesive bare sandy substrate, free of living material. The sediment was sieved through a 2-mm mesh size to obtain the coarse-grained sand fraction and stored in PVC boxes at Kristineberg Marine Research Station until the experiment was set up. Sediment was distributed in 16-cm diameter cores (20 cm deep). In each of the cores, a single method was installed, with five independent replicates per method: plates (without string, with string, and with string and buoy) at ~15 cm depth and bars, in the flume experiment, digging 4 cm in the sediment and leaving 11 cm above; and 15 cm in the sediment and leaving 15 cm above the field experiment (see Fig. 1a).

The cores were positioned in the test section and carefully inserted in the test section and adjusted to fill any remaining gap, producing a continuous bed of homogeneous mobile sediment, to ensure the sediment surface was level and parallel to the bottom of the flume (Fig. 1). For each hydrodynamic condition, one core of each method was tested simultaneously. The hydraulic flume was set up according to the type of hydrodynamic forces required for each run experiment (i.e., unidirectional or oscillatory), as explained previously. The flume design ensures hydrodynamic independence among measurement points (Infantes et al. 2021). This setup

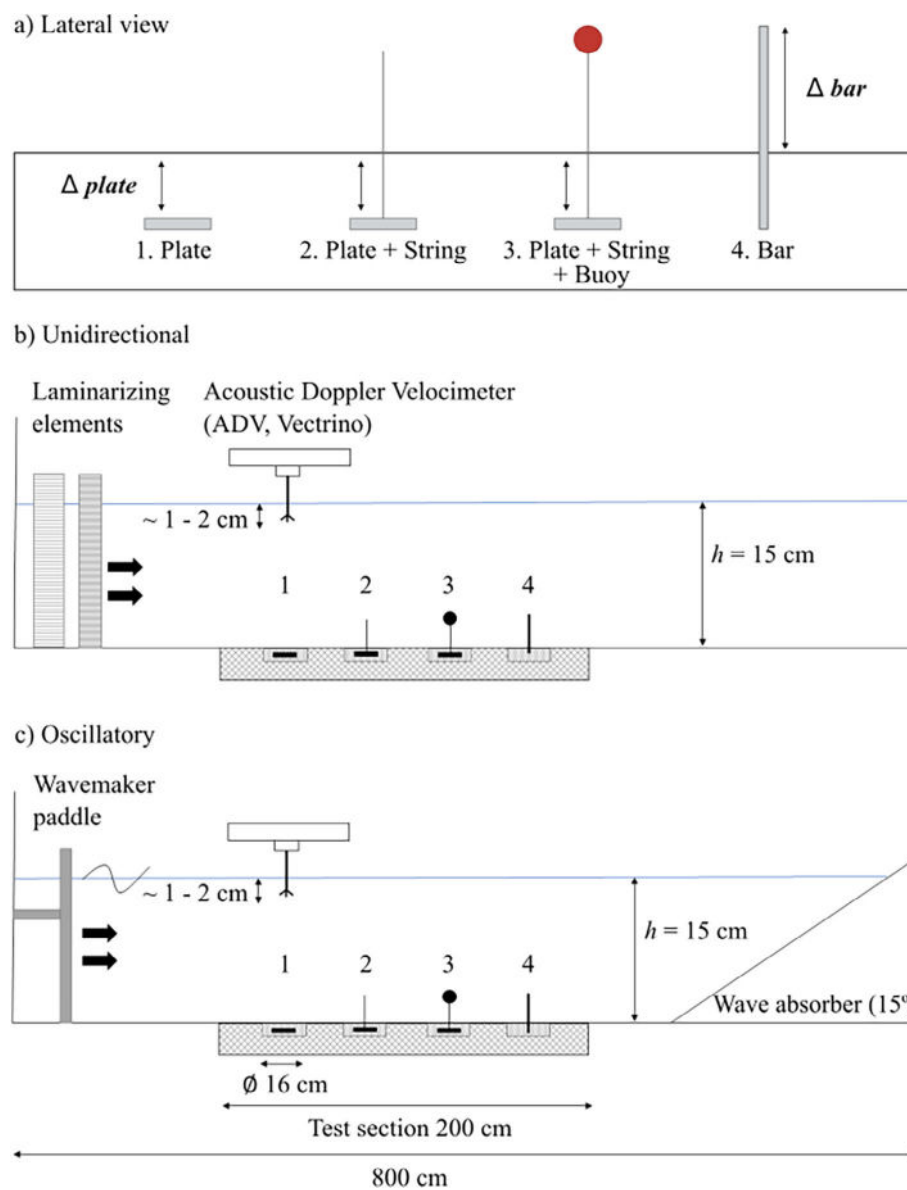


**Fig. 1.** Diagram of the bed-level measurement tools and experimental setup. (a) Lateral view of the bed-level measurement tools, including (1) plate, (2) plate + string, (3) plate + string + buoy, and (4) steel rebar ( $\varnothing 1$  cm), each placed in a separate core in the test section. The surrounding area was filled with gravel to prevent the mobilization of sediment by hydrodynamic forces. The elevation changes were measured according to the method used, that is, from the plate to the sediment surface or from the sediment surface to the top of the bar, respectively. Experimental setup of the hydraulic flume used to test sediment-level monitoring methods under (b) unidirectional flow and (c) oscillatory flow regimes. Flow velocities were measured using an Acoustic Doppler Velocimeter positioned 1–2 cm below the water surface. The flume ( $8 \times 0.5 \times 0.5$  m) included laminarizing elements and a wave paddle system to simulate current and wave conditions. Illustrations are not to scale; see Infantes et al. (2021) for full flume specifications.

was repeated in five independent experimental runs for unidirectional flow and for oscillatory flow, respectively. For each experimental run, each sample core was exposed to two stepwise increases in flow velocities, first  $11 \text{ cm s}^{-1}$  and after 30 min increased to  $23 \text{ cm s}^{-1}$  for 30 min, which is a standard method in hydraulic flumes to estimate erosion (e.g., Ganthy et al. 2015; Infantes et al. 2022; Jacobs et al. 2011). The characteristic flow velocity for the two experimental hydrodynamic conditions corresponded with the range of velocities

found in the field, simulating natural calm and storm conditions (Pereda-Briones et al. 2018).

Sediment level before and after each increment in flow velocity was measured as the vertical distance between the sediment surface and the reference element (plate or bar) using a metal ruler with  $\pm 1$  mm accuracy. The volume of sediment within each cylindrical core was calculated before and after each experimental run using Eq. 3. The total erosion rate ( $\text{cm h}^{-1}$ ) was then determined from the difference in sediment volume

from the baseline (initial measurement) and that recorded after each 1-h hydrodynamic exposure at each experiment run.

$$V = \pi r^2 h \quad (3)$$

where  $r^2$  is the radius of the core and  $h$  is the measured height of the sediment in the core, regarding the method used (see Fig. 1a).

The resolution of the experimental design was quantified as the minimum detectable difference (MDD) in bed-level change, estimated as twice the standard deviation of relative erosion across replicate cores. Under current-driven flume conditions, the MDD in bed-level change was approximately 1.89 mm, whereas under wave-driven conditions, it was 2.49 mm. Accordingly, differences among methods smaller than this threshold cannot be resolved under the present experimental design.

While the flume provided controlled hydrodynamic forcing and a sediment bed leveled to form a continuous surface, no fixed reference was available to define or independently verify an absolute benchmark of bed-level change. Accordingly, the flume experiments were designed as a controlled comparative framework to assess relative consistency and precision among methods under identical forcing conditions. The resolution of the experimental design is constrained by measurement uncertainty and variability among replicate cores, which together determine the MDD in bed-level change and are considered a limitation. In addition, measurements were referenced to the local sediment surface, and small-scale bedforms (e.g., ripples) may introduce variability in absolute erosion estimates. This source of variability affects all methods similarly and is therefore not expected to bias relative comparisons among tools, although it is considered a limitation when interpreting absolute erosion rates.

### Assessment of turbulence induced by structural elements

To evaluate whether the structural elements of the methods tested in the experimental setup (i.e., string, buoy and bar) could potentially generate turbulence affecting bed erosion results, the Reynolds number (Re) was calculated for each element. The Reynolds number describes the ratio of inertial to viscous forces in the flow and indicates whether the flow around an object is likely to produce turbulent wakes (Ortiz and Klompmaker 2015):

$$\text{Re} = \frac{U^* \delta_{\text{fluid}}^* d}{\mu_{\text{fluid}}} \quad (4)$$

where  $U$  corresponded to the mean flow velocity in the flume ( $U = 0\text{--}23 \text{ cm s}^{-1}$ ),  $\rho_{\text{fluid}}$  corresponded to the seawater density ( $\rho_{\text{fluid}} = 1020.36 \text{ kg m}^{-3}$ ),  $d$  corresponded to the diameter of the elements (string = 0.008 m, buoy = 0.04 m, bar = 0.01 m) and  $\mu_{\text{fluid}}$  corresponded to the seawater viscosity ( $\mu_{\text{fluid}} = 1.206 \times 10^{-3} \text{ Pa s}^{-1}$ ).

Secondly, to evaluate the residual turbulence potentially transmitted to the sediment surface, we approximated the wake delay (Pope 2000):

$$u'(z) \sim U \left( \frac{d}{z} \right)^n \quad (5)$$

where  $u'(z)$  is the residual turbulence fluctuation at distance  $z$  from the object,  $z$  is the vertical distance from the object to the bottom,  $d$  is the diameter of the object, and  $n$  is an empirical exponent describing near-wake ( $n = 1$ ) and far-wake ( $n = 2$ ) conditions (Tennekes and Lumley 1972; Pope 2000). Evaluating both regimes provides an order-of-magnitude estimate of the additional bed shear stress potentially induced by structural elements. The associated bed shear stress was approximated as for current (Eq. 6a) and wave (Eq. 6b) conditions (Wiberg and Smith 1983):

$$\tau_{\text{current}} = \rho u_*^2 \quad (6a)$$

$$\tau_{\text{wave}} = \frac{1}{2} \rho u_*^2 \quad (6b)$$

where  $\rho$  is water density ( $\rho_{\text{fluid}} = 1020.36 \text{ kg m}^{-3}$ ), and  $u_*$  is the shear velocity, approximated as  $u'(z)$ .

Orbital velocity, wave friction factor and bed roughness terms were not explicitly resolved. Consequently, these calculations are intended as order-of-magnitude estimates for relative comparison among methods under identical hydrodynamic forcing, rather than as absolute estimates of near-bed shear stress.

### Field validation in an eelgrass meadow

To evaluate the validity of the laboratory results experiment conducted under controlled flume conditions, field trials were conducted in a *Zostera marina* meadow in the estuary of the Bay of Santander estuary, Spain ( $43^\circ 26' 48.8'' \text{N}$ ,  $3^\circ 46' 28.2'' \text{W}$ ,  $22.7 \text{ km}^2$ ) (Fig. 2a). The study area is a tidal flat, gently sloping, sandy-muddy sedimentary area predominantly covered by extensive *Z. noltei* meadows ( $\sim 454 \text{ ha}$ ), interspersed with patches of *Z. marina* ( $\sim 57 \text{ ha}$ ) found in both intertidal and shallow subtidal zones (Ondiviela et al. 2015), and harbors the largest share of *Z. marina* meadows in the Iberian Peninsula (61.5%,  $5.8 \text{ km}^2$  across 48 meadows) (García-Redondo et al. 2019). While this experiment focused on *Z. marina*, some of the patches evaluated during the surveys also contained *Z. noltei*. In those cases, we estimated the cover of both *Zostera* species. In the summer of 2023, during the peak growing season, average seagrass shoot density was  $2060 \pm 638 \text{ shoots m}^{-2}$  (mean  $\pm$  SD).

### Field deployment and sediment level monitoring

The three methods (plate + string, plate + string + buoy, and bars) were deployed in replicates of three across three treatments: outside the meadow (bare sediment), meadow

edge, and within the meadow (Fig. 2b,c) to test if the methods were similar under different habitat types.

Plates were deployed following a modified method from Marin-Diaz et al. (2025), which itself was adapted from Bell et al. (1999). A sediment layer was lifted with a spade to minimize disturbance to the meadow and sediment structure during deployment. The plate was placed at the bottom of the excavated area (~ 10–15 cm depth), and the sediment carefully re-filled. In parallel, bars (30 cm long) were vertically inserted into the sediment using a hammer, leaving ~ 15 cm exposed. Sediment level was measured using a metal ruler with  $\pm 0.1$  cm accuracy, recording plate burial depth and/or bar exposure. Plate burial depth was measured from the plate to the sediment surface, and bar exposed length from the top of the bar to the sediment surface (see Fig. 1a). Sediment level from each device (plate or bar) was measured at the time of deployment (baseline measure) and at four additional times during the following year (between May 2023 and March 2024). Three replicate measurements were taken for each device and sampling event and averaged to minimize sampling error and observer bias. All fieldwork was performed during low tide.

In this study, each sediment level value was calculated as the sequential difference between consecutive sampling events ( $\Delta$ Sediment elevation =  $Elevation_t - Elevation_{t-1}$ ), and averaged at a particular time point. This approach ensures that each

measurement represents an independent estimate of short-term sediment elevation change, rather than an absolute measure of bed elevation.

Sediment particle distribution ( $d_{50}$ ,  $\mu\text{m}$ ) followed a consistent pattern across most sites, with coarse sand (250–1000  $\mu\text{m}$ ) being the dominant fraction (Supporting Information Table S5).

### Statistical analysis

For laboratory data, we used linear models to assess the effect of the method used (four levels), flow velocity (two levels) and their interaction on the response variable surface sediment erosion. We fitted a different model for unidirectional and oscillatory flow, respectively. Assumptions of normality and homogeneity of variances were verified through inspection of residuals and the Shapiro–Wilk test and Levene’s test, respectively. To identify statistically significant differences among methods under each flow condition, pairwise comparisons of estimated marginal means were computed using the *emmeans* package, with Tukey’s HSD post hoc test using the *multcomp* package (Hothorn et al. 2008). Estimated differences and associated confidence intervals were examined to assess the magnitude and uncertainty of differences among methods. The significance level ( $\alpha$ ) set for all tests was 0.05. Letters above bars in plots indicate significant differences among treatments for each experimental flow condition.

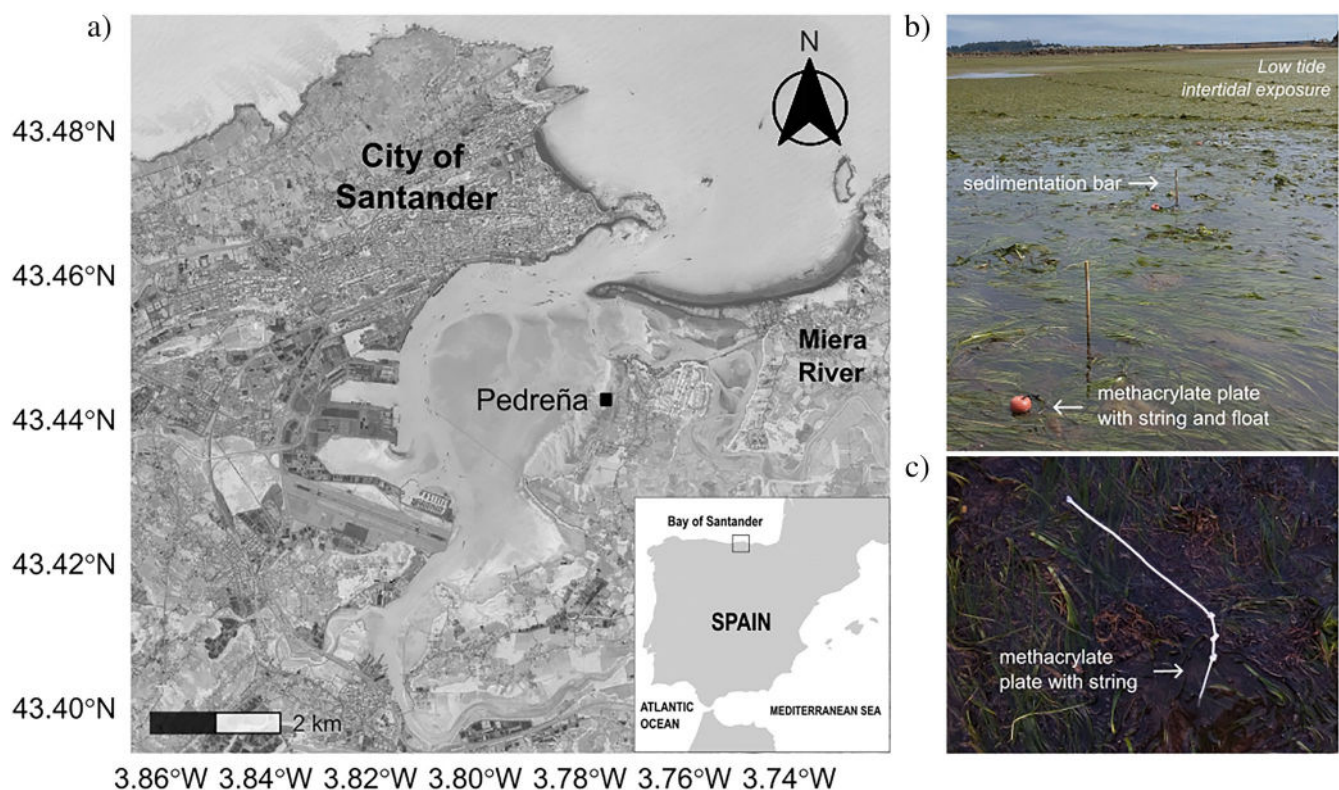


**Fig 2.** (a) Location of the study area in the Bay of Santander (northern Spain) showing sampling sites with *Zostera marina* meadows (Pedreña). Image from Copernicus Hub. (b, c) Field deployment of bars and plates during low tide.

For field data, differences between bed-level tools on elevation change response were tested using generalized linear models. The response variable, “sediment elevation change,” was calculated as the sequential difference in elevation between consecutive sampling events, obtained from sedimentation plates or bars (see previous section). Variables included “method” (categorical with three levels: plate + string, plate + string + buoy, and bar), and “habitat” (categorical with three levels: bare sediment, meadow edge and inside the meadow), as well as their interaction (“method” × “habitat”). Post hoc pairwise comparisons of estimated marginal means were conducted using the *emmeans* package, with Tukey’s HSD adjustment applied via the *multcomp* package (Hothorn et al. 2008) to identify level-specific differences among model levels. We validated model performance and checked model assumptions by inspecting residuals Q–Q plots (Harrison et al. 2018). We further evaluated model fit using the *performance* package (Lüdtke et al. 2021). Data are shown as means ± standard error. All analyses were computed in R version 4.5.1 (R Core Team 2025).

## Assessment

### Flume experiments: Unidirectional and oscillatory flow

Erosion rates did not differ significantly among methods under unidirectional or oscillatory flow at either low or high velocities ( $p > 0.1$ , Fig. 3 and Table 1), with observed differences remaining below the resolution of the experimental design (i.e., MDD = 1.89 mm under current conditions, and 2.49 mm under wave-driven conditions). Erosion rates increased with flow velocities ( $p < 0.05$ ; Table 1), reaching approximately 40–90 cm<sup>3</sup> h<sup>-1</sup> under current-driven flow and 20–80 cm<sup>3</sup> h<sup>-1</sup> under wave-driven conditions at higher velocities (Supporting Information Figs. S3, S4). Additionally, ripple formation was observed with increasing wave forcing under both flow conditions (Supporting Information Fig. S5). Estimated marginal means showed no significant differences between treatments at either flow level (Supporting Information Tables S1–S4).

### Effect of structural elements on flow and turbulence

The Reynolds numbers associated with the flow-object interaction remained low for the string and the bar (Table 2). The buoy reached higher values ( $Re \approx 7591$ ), which could generate a local turbulent wake. Based on simplified wake-decay formulations, turbulent velocity fluctuations at the sediment surface (11 cm below the buoy) were estimated to range between 0.03 and 0.08 m s<sup>-1</sup>. These fluctuations corresponded to order-of-magnitude estimates of additional bed shear stress of approximately 0.001–0.007 N m<sup>-2</sup> under current-drive conditions ( $\tau_{\text{current}}$ ) and 0.0005–0.0035 N m<sup>-2</sup> under wave-driven conditions ( $\tau_{\text{wave}}$ ).

Representative example calculations are provided in the Supporting Information to illustrate the rough estimates described above.

### Field validation and method comparison

We did not find an effect on the method used to assess sediment elevation change in the field (i.e., plate + string, plate + string + buoy, and bar) (Fig. 4; Table 3). We did not find an interactive effect of method × position along the sand-seagrass gradient, either. In contrast, we did find a significant effect of the position where bars or plates were installed across habitats (bare sediment, meadow edge, inside meadow) (Table 3). In particular, lower sediment elevation change (i.e., greater stability) was found inside seagrass meadows compared to the meadow edge and to the bare sediment (Table 3), regardless of the tool used. Overall, variability was mainly explained by habitat rather than by the monitoring technique (Fig. 4; Table 3). This pattern is consistent with the capacity of seagrass meadows to attenuate wave energy and modify near-bed hydrodynamics, which can influence sediment stability and bed-level change (Infantes et al. 2012).

## Discussion

In this study, we validate two cost-effective field tools for measuring short-term sediment elevation changes in shallow coastal habitats. All four tool configurations tested (i.e., plate, plate + string, plate + string + buoy, and bar) produced comparable estimates of sediment elevation change under both controlled and natural hydrodynamic conditions, confirming their comparability and interchangeability across flow regimes and habitats. Under controlled conditions, erosion outcomes were consistent regardless of hydrodynamic force (unidirectional vs. oscillatory) and flow velocity regime (11 vs. 23 cm s<sup>-1</sup>). No detectable differences between tools were observed within the resolution of the experimental design (MDD  $\approx$  1.9 mm for current-driven and 2.5 mm for wave-driven conditions). Although the buoy generated localized turbulence, the associated shear stress estimates indicated a limited additional hydrodynamic influence relative to background forcing. Field validation in *Z. marina* meadow further supported the consistency among these tools, indicating that patterns in sediment elevation change were primarily driven by habitat type (i.e., bare sediment, meadow edge, and within the meadow). These results ensure data reliability and highlight the flexibility to select or combine the most appropriate method according to site-specific environmental and logistical constraints for in situ ecological studies.

In addition, our results indicated that the use of buoys or strings do not measurably affect relative erosion outcomes among the tested methods under the experimental conditions. At sufficiently high Reynolds numbers, boundary-layer turbulence generates random velocity fluctuations, and sediment erosion occurs once the bed shear stress ( $\tau_b$ ) exceeds a

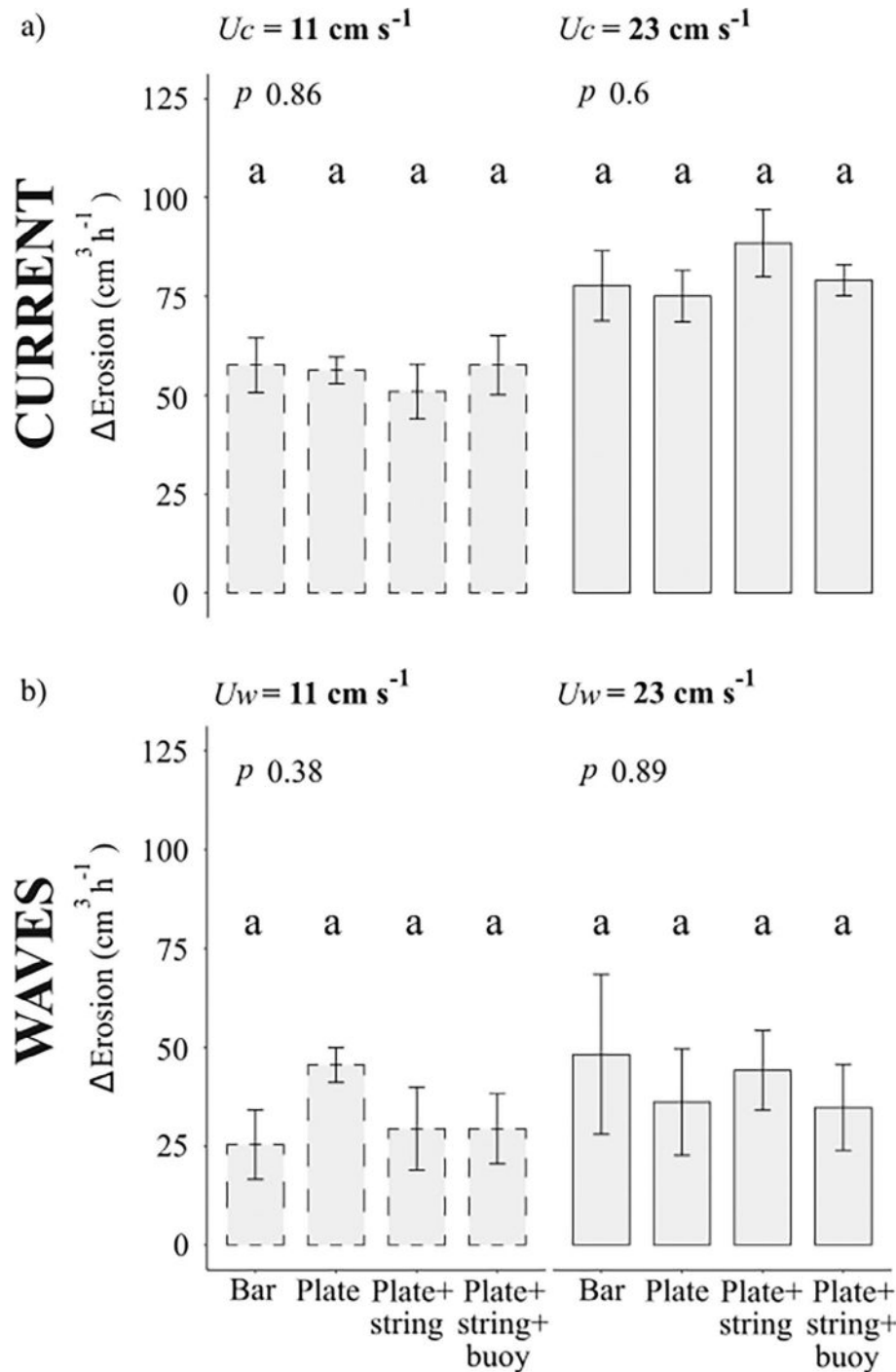


**Fig. 3.** Mean ( $\pm$  SE) sediment erosion rate ( $\text{cm}^3 \text{h}^{-1}$ ) for the four bed-level monitoring methods under (a) unidirectional ( $U_c = 11$  and  $23 \text{ cm s}^{-1}$ ) and (b) oscillatory ( $U_w = 11$  and  $23 \text{ cm s}^{-1}$ ) flow conditions. Each barplot represents  $n = 5$  replicates cores per treatment. Letters above bars indicate significant differences among methods in each flow energy treatment based on Tukey HSD ( $p$ -value  $< 0.05$ ). No significant differences were detected among methods at either flow regime.

critical threshold (Soulsby and Damgaard 2005). Despite the buoy generated local turbulent flow at a higher velocity ( $23 \text{ cm s}^{-1}$ ,  $Re \approx 7800$ ), its effect decayed rapidly with the bed distance from the buoy. Order-of-magnitude estimates suggest

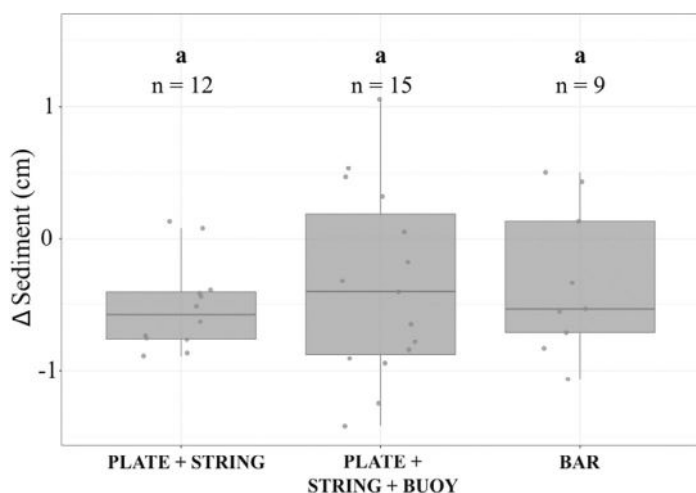
that residual turbulence at the sediment surface ( $0.03$ – $0.08 \text{ N m}^{-2}$  at  $11 \text{ cm}$  above the bed) represents only a limited additional contribution to bed shear stress relative to background forcing in bare sediments ( $0.2$ – $0.3 \text{ N m}^{-2}$ , e.g.,

**Table 1.** Sediment erosion under unidirectional and oscillatory flow conditions. Two-way ANOVAs testing the effects of method and flow velocity, degrees of freedom (df), *F*-values, and *p*-values are shown.

	Unidirectional flow			Oscillatory flow		
	df	<i>F</i> -value	<i>p</i> -value	df	<i>F</i> -value	<i>p</i> -value
Method	3	0.2179	0.8832	3	0.5780	0.6337
Flow velocity	1	4.3269	0.0456	1	1.8873	0.1791
Method × flow velocity	3	0.8253	0.4897	3	0.6939	0.5626
Residuals	32			32		

**Table 2.** Reynolds numbers (Re) calculated for the structural elements of each monitoring method under two flow velocities (11 and 23 cm s<sup>-1</sup>). Re values indicate flow regime and potential turbulence generation for each element. N/A: Re not applicable as the element remained buried.

Element	Diameter (ø, m)	Re by flow velocity (cm s <sup>-1</sup> )	
		11	23
Plate	N/A	N/A	N/A
Plate + string	0.004	361.4	759.1
Plate + string + buoy	0.04	3614.4	7590.9
Bar	0.01	903.6	1982.3

**Fig. 4.** Effect of monitoring method (plate + string, plate + string + buoy, bar) on sediment elevation change (cm) in *Zostera marina* meadows. Different lower-case letters above each box indicate significant differences (*p*-value < 0.05, Tukey HSD post hoc tests). The number of individual sediment monitor elements/units is shown below each letter.

Soulsby 1997; Widdows et al. 2008; Hansen and Reidenbach 2012). Because these estimates are based on simplified wake-decay and shear-stress formulations, they should be interpreted cautiously and not as site-specific threshold exceedance

tests. The string and bar consistently remained in low-Re regimes where wake-induced turbulence was minimal. Importantly, all structural elements were exposed to identical hydrodynamic forcing, and any uncertainty associated with turbulence estimation therefore applies equally across methods. Thus, the comparative consistency among erosion measurements reflects differences in tool configuration rather than artifacts introduced by deployment-related elements. None of the structural elements introduced in the flume contributed to sediment erosion, therefore validating experimental outcomes. This result is key as strings or bars are critical elements deployed for easier retrieval of the plate, and the buoy adds an extra element to find the string by preventing its burial, especially in subtidal conditions.

Shallow water depths and bottom stress induced by waves (i.e., oscillatory flow) and currents (i.e., unidirectional flow) control sediment transport, being the main drivers for morphological adjustments and surface elevation changes, including seagrass habitats where oscillatory flow affects both bed-load transport and sediment resuspension (Soulsby et al. 1993; Marin-Diaz et al. 2020). During the flume experiment, sediment erosion increased at higher flow velocities as expected (Fig. 3; Table 1), both under unidirectional and oscillatory flow (Supporting Information Figs. S3, S4). Notably, we observed the formation of small sand ripples (bedforms) under high hydrodynamic conditions (currents and waves, 23 cm s<sup>-1</sup>, Supporting Information Fig. S5). When water flowing over sand exceeds the critical shear stress for motion, the first bedforms to develop are current ripples (Bartholdy et al. 2015). Sand ripples are associated with net sediment transport, as ripple migration represents a key mode of bedload transport, with most sediment movement occurring within a few centimeters of the bed (Coleman and Melville 1996; Wang and Yuan 2018). Since the dynamics of ripples were beyond the scope of this study, they were not measured or investigated. However, this constitutes a limitation, as ripple-scale bedforms may affect absolute bed-level change estimates. Nevertheless, future applications could reduce these sources of uncertainty by using reference devices that bridge across local bed relief (e.g., flat disk or a flat ruler on top of the bed to measure the distance from the bed to the bar top), or by combining these

**Table 3.** Effects of habitat, monitoring method, and their interaction on sediment elevation change in *Z. marina* meadows. Degrees of freedom (df), *F*-value, and *p*-values are shown.

Response	Variables	df	<i>F</i> -value	<i>p</i> -value
Sediment elevation change	Habitat	2	10.0359	<0.001***
	Methods	2	0.1978	0.8217
	Method : Habitat	4	0.2342	0.9166

\*\*\**p* < 0.001.

tools with independent benchmarks or high-precision positioning techniques (e.g., Real-Time Kinematic Differential Global Positioning System).

Regarding the existing methods to quantify sediment elevation changes in coastal settings, each differs in materials, precision, applicability and practicality (e.g., Arias-Ortiz et al. 2018; Cahoon and Turner 1989; Callaway et al. 1996; French and Burningham 2003; Lewis and McGlathery 2023; Murray et al. 2019; Stokes et al. 2010; Thomas et al. 2002). While conventional approaches yield valuable data (e.g., SET, sedimentation-erosion bar, MH, electronic devices, or isotopic techniques), they are often expensive, labor-intensive, prone to corrosion, fragile in the field, and require specialized equipment or delicate components requiring regular maintenance (Cahoon et al. 2002a; Thomas and Ridd 2004). In this study, we focused on sedimentation plates and bars, validating their performance as reliable tools for measuring short-term (monthly, yearly) sediment elevation changes, as they produced consistent results under field conditions (Fig. 4; Table 3). Sedimentation plates (0.7–1.1 €) and bars (2–15 €) provide a lightweight and robust, and maintenance-free alternative. The simple and low-cost design facilitates transport, deployment and recovery using visual markers (e.g., strings, buoys) in a range of dynamic sedimentary environments. They enable extensive spatial replication and high-resolution monitoring, effectively compensating for potential measurement uncertainty and minimizing data loss if individual units are displaced or damaged (see Recommendations, Table 4).

Despite their advantages, some limitations should be acknowledged. During the deployment, plates must be positioned horizontally and bars vertically to ensure consistent reference geometry, as deviations may lead to small measurement errors. Previous studies reported variable performance depending on material and habitat. In biologically active unvegetated areas, bioturbation may partially bury or displace the plates (Marin-Diaz et al. 2025). Stokes et al. (2010) found limited success using small metal plates in mangrove zones due to biological interferences, whereas Lewis and McGlathery (2023) and Marin-Diaz et al. (2025) successfully applied sediment plates in seagrass settings. Other studies applied sediment plates in combination with other

techniques, like SETs and <sup>137</sup>Cs sediment cores dating (French and Burningham 2003). Similarly, while UAV-based Structure-from-Motion techniques offer centimeter-scale spatial resolution and flexible deployment, their application in aquatic environments is limited by water-surface dynamics and optical constraints (e.g., Johansen et al. 2022; Gray et al. 2022; Duffy et al. 2018; Novo et al. 1989). Moreover, ground-truthing through in situ measurements remains essential to validate remotely derived data. These approaches therefore complement, rather than replace, simple in situ bed-level tools (e.g., Balke et al. 2021; AlObaidi and Valyrakis 2021). In organic-rich environments, fouling on strings, buoys, or bars can reduce marker visibility or alter buoyancy (authors' observations). Although these are non-invasive tools, care should be taken to minimize disturbance to vegetation and preserve sediment integrity during installation. Furthermore, these methods do not quantify suspended sediment concentration or fluxes of associated materials (e.g., organic matter, nutrients, or grain size), which requires complementary methods such as sediment traps (Nolte et al. 2013).

To our knowledge, no previous inter-comparison of sediment plate and bar measurement methods has been published. This study provides a practical cross-validation under both controlled and natural conditions for sedimentation plates (alone, with a string, or with a string and buoy) and bars as reliable and combinable tools for monitoring in situ sediment dynamics in coastal environments (Figs. 3, 4, Tables 1–3). As ecosystem engineers become central to coastal restoration and ecosystem service frameworks (Byers et al. 2006; Temmink et al. 2020), the use of standardized tools is critical for evaluation and management of coastal interventions. Future applications are particularly valuable to address key ecological and management questions, such as i) how biological processes (e.g., bioturbation, growth plant patterns, response to burial) influence sediment accretion, erosion, and surface-elevation changes in tidal flats, marshes, seagrass meadows, algal mats, or benthic fauna such as oyster beds; (ii) how vegetation structure modulates sedimentation and stabilization dynamics under storm conditions or human disturbances or (iii) how much coastal ecosystems restoration or conservation actions can contribute to mitigate climate change threats, sea level rise or increase in frequency and intensity of storms, through enhancing sediment stabilization and accretion. However, cohesive and mixed beds require further testing to warrant the reliability of the sediment response outcomes.

### Comment and recommendations

The applicability of the findings presented in this study is constrained to shallow coastal environments with sandy, non-cohesive substrates and to a seagrass-dominated estuarine system, and should be interpreted within this environmental

**Table 4.** Summary of the main advantages, limitations, and recommended applications for the four sediment monitoring methods. Each method is evaluated by suitability to environment, field practicality, and potential limitations under intertidal and subtidal conditions. Recommended uses are based on flume validation and field performance.

Method	Environment	Advantages	Disadvantages	Recommendations/ observations
Sedimentation plate (buried)	Intertidal, subtidal	Not visible once installed Low risk of disturbance	Requires external markers or an accurate GPS to find Risk of loss if not well referenced	Not recommended for field studies, just suitable in areas with a high risk of disturbance
Sedimentation plate + string	Intertidal zones	Relatively unobtrusive but easy to find	String may be disturbed or attract attention	Recommended for recreational beaches or tourism areas
Sedimentation plate + string + buoy	Subtidal, deeper water	A buoy as a fixed marker ensures localization under low-visibility systems Suitable for divers	The buoy is highly visible, prone to disturbance by people, boats, or fishing gear It may be dragged or cut by anchors or propellers in high-use areas Biofouling could affect the buoy's buoyancy	Remove biofouling during each monitoring survey Extreme weather conditions may alter performance outcomes (e.g. turbulence, potential loss of deployed elements)
Sedimentation bar	All systems	Resistant, suitable for complex or dynamic environments	Risk of displacement by anchors, trawling, or fishing Less manageable than plates; more difficult to deploy/maintain	Use as a complementary method in field-exposed ecosystems Not recommended in frequent human transit areas due to safety hazard (e.g., risk of injury if accidentally stepped on or encountered by swimmers)

scope. The influence of small-scale bedforms (e.g., ripples) represents a limitation for absolute sediment change estimates, but does not undermine relative comparisons among methods. To overcome the limitations in dynamic, intertidal, shallow, or human-used coastal settings, we encourage their combined use, which can enhance the resolution, robustness, and replicability of measurements. Further testing to warrant performance outcomes under extreme weather conditions is needed. Recommended uses are based on flume validation and field performance, reducing methodological uncertainty and strengthening the confidence of the low-cost bed-level tools evaluated.

### Author Contributions

Lucía Rodríguez-Arias conducted the review, simulations in the flume and in the field experiment, performed data curation and formal analyses, and wrote the manuscript. Inés Mazzarasa contributed to the study design and methodology in the field experiment and assisted with manuscript revision. Beatriz Marin-Diaz, Teresa Alcoverro, Barbara Ondiviela, and Jordi F. Pagès contributed to conceptual development, methodological refinement, reviewed and edited drafts. Eduardo Infantes supervised the work, contributing to conceptualization and methodology, and reviewed and edited manuscript

drafts. Teresa Alcoverro and Eduardo Infantes acquired funding.

### Acknowledgments

The research leading to these results received funding from the Spanish National Project (AEI-MICINN), grants STORM (PID2020-113745RB-I00), and DYNCOAST (PID2023-151732OA-I00), funded by MCIN/AEI/10.13039/501100011033 and the FES+. LRA was funded by the FPI fellowship (PRE2021-099061), financed by MCIN/AEI/10.13039/501100011033 and the FES+. Beatriz Marin-Diaz was supported by a “Margalida Comas” post-doctoral contract co-funded by the Council of European Funds and the Government of the Balearic Islands. Warm thanks to Marit Classen and Ali Ademi for their laboratory assistance. We also thank Kristineberg Center and their staff for the use of their facilities and their kind attention.

### Conflicts of Interest

None declared.

### Data Availability Statement

Data and R code that support the findings of this study are archived in Zenodo: <https://doi.org/10.5281/zenodo.18599075>.

## References

- AlObaidi, K., and M. Valyrakis. 2021. "Linking the Explicit Probability of Entrainment of Instrumented Particles to Flow Hydrodynamics." *Earth Surface Processes and Landforms* 46, no. 12: 2448–2465. <https://doi.org/10.1002/esp.5188>.
- Arias-Ortiz, A., P. Masqué, J. Garcia-Orellana, et al. 2018. "Reviews and Syntheses: 210Pb-Derived Sediment Carbon Accumulation Rates in Vegetated Coastal Ecosystems – Setting the Record Straight." *Biogeosciences* 15: 6791–6818. <https://doi.org/10.5194/bg-15-6791-2018>.
- Balke, T., A. Vovides, C. Schwarz, G. L. Chmura, C. Ladd, and M. Basyuni. 2021. "Monitoring Tidal Hydrology in Coastal Wetlands with the 'Mini Buoy': Applications for Mangrove Restoration." *Hydrology and Earth System Sciences* 25, no. 3: 1229–1244. <https://doi.org/10.5194/hess-25-1229-2021>.
- Bartholdy, J., V. B. Ernsten, B. W. Flemming, C. Winter, A. Bartholomä, and A. Kroon. 2015. "On the Formation of Current Ripples." *Scientific Reports* 5: 11390. <https://doi.org/10.1038/srep11390>.
- Beca-Carretero, P., S. Varela, and D. B. Stengel. 2020. "A Novel Method Combining Species Distribution Models, Remote Sensing, and Field Surveys for Detecting and Mapping Subtidal Seagrass Meadows." *Aquatic Conservation: Marine and Freshwater Ecosystems* 30, no. 6: 1098–1110. <https://doi.org/10.1002/aqc.3312>.
- Bell, S. S., B. D. Robbins, and S. L. Jensen. 1999. "Gap Dynamics in a Seagrass Landscape." *Ecosystems* 2, no. 6: 493–504. <https://doi.org/10.1007/s100219900097>.
- Blum, M. D., and H. H. Roberts. 2009. "Drowning of the Mississippi Delta Due to Insufficient Sediment Supply and Global Sea-Level Rise." *Nature Geoscience* 2, no. 7: 488–491. <https://doi.org/10.1038/ngeo553>.
- Boumans, R. M. J., and J. W. Day. 1993. "High Precision Measurements of Sediment Elevation in Shallow Coastal Areas Using a Sedimentation-Erosion Table." *Estuaries* 16, no. 2: 375. <https://doi.org/10.2307/1352509>.
- Brown, J., A. Colling, D. Park, J. Phillips, D. Rothery, and J. Wright. 1995. "An Introduction to Shallow-Water Environments and Their Sediments." In *Waves, Tides and Shallow-Water Processes*, edited by G. Bearman, 72–94. Open University.
- Butman, B., M. Noble, and D. W. Folger. 1979. "Long-Term Observations of Bottom Current and Bottom Sediment Movement on the Mid-Atlantic Continental Shelf." *Journal of Geophysical Research* 84, no. C3: 1187–1205. <https://doi.org/10.1029/JC084iC03p01187>.
- Byers, J. E., K. Cuddington, C. G. Jones, et al. 2006. "Using Ecosystem Engineers to Restore Ecological Systems." *Trends in Ecology & Evolution* 21, no. 9: 493–500. <https://doi.org/10.1016/j.tree.2006.06.002>.
- Cabaço, S., R. Santos, and C. M. Duarte. 2008. "The Impact of Sediment Burial and Erosion on Seagrasses: A Review." *Estuarine, Coastal and Shelf Science* 79, no. 3: 354–366. <https://doi.org/10.1016/j.ecss.2008.04.021>.
- Cahoon, D. R., J. C. Lynch, P. Hensel, et al. 2002a. "High-Precision Measurements of Wetland Sediment Elevation: I. Recent Improvements to the Sedimentation-Erosion Table." *Journal of Sedimentary Research* 72, no. 5: 730–733. <https://doi.org/10.1306/020702720730>.
- Cahoon, D. R., J. C. Lynch, B. C. Perez, et al. 2002b. "High-Precision Measurements of Wetland Sediment Elevation: II. The Rod Surface Elevation Table." *Journal of Sedimentary Research* 72, no. 5: 734–739. <https://doi.org/10.1306/020702720734>.
- Cahoon, D. R., and R. E. Turner. 1989. "Accretion and Canal Impacts in a Rapidly Subsiding Wetland II. Feldspar Marker Horizon Technique." *Estuaries* 12, no. 4: 260–268. <https://doi.org/10.2307/1351905>.
- Callaway, J. C., J. A. Nyman, and R. D. DeLaune. 1996. "Sediment Accretion in Coastal Wetlands: A Review and a Simulation Model of Processes." *Current Topics in Wetland Biogeochemistry* 2, no. 2: 23.
- Chanson, H. 2004. "Hydraulics of Rectangular Dropshafts." *Journal of Irrigation and Drainage Engineering* 130, no. 6: 523–529. [https://doi.org/10.1061/\(ASCE\)0733-9437\(2004\)130:6\(523\)](https://doi.org/10.1061/(ASCE)0733-9437(2004)130:6(523)).
- Coleman, S. E., and B. W. Melville. 1996. "Initiation of Bed Forms on a Flat Sand Bed." *Journal of Hydraulic Engineering* 122: 301–310. [https://doi.org/10.1061/\(asce\)0733-9429\(1996\)122:6\(301\)](https://doi.org/10.1061/(asce)0733-9429(1996)122:6(301)).
- Duffy, J. P., L. Pratt, K. Anderson, P. E. Land, and J. D. Shutler. 2018. "Spatial Assessment of Intertidal Seagrass Meadows Using Optical Imaging Systems and a Lightweight Drone." *Estuarine, Coastal and Shelf Science* 200: 169–180. <https://doi.org/10.1016/j.ecss.2017.11.001>.
- Einstein, H. A., A. G. Anderson, and J. W. Johnson. 1940. "A Distinction Between Bed-Load and Suspended Load in Natural Streams." *Eos, Transactions American Geophysical Union* 21: 628–633. <https://doi.org/10.1029/TR021i002p00628>.
- French, J. R., and H. Burningham. 2003. "Tidal Marsh Sedimentation Versus sea-Level Rise: A Southeast England Estuarine Perspective." In *Proceedings of the International Conference on Coastal Sediments 2003*, edited by R. A. Davis, 1–14. Corpus Christi, Tex: World Scientific Publishing and East Meets West Productions.
- Ganthy, F., L. Soissons, P.-G. Sauriau, R. Verney, and A. Sottolichio. 2015. "Effects of Short Flexible Seagrass *Zostera noltei* on Flow, Erosion and Deposition Processes Determined Using Flume Experiments." *Sedimentology* 62, no. 4: 997–1023. <https://doi.org/10.1111/sed.12170>.
- García-Redondo, V., I. Bárbara, and P. Díaz-Tapia. 2019. "Zostera marina Meadows in the Northwestern Spain: Distribution, Characteristics and Anthropogenic Pressures." *Biodiversity and Conservation* 28: 1743–1757. <https://doi.org/10.1007/s10531-019-01753-4>.
- Gera, A., J. F. Pages, R. Arthur, et al. 2014. "The Effect of a Centenary Storm on the Long-Lived Seagrass *Posidonia oceanica*." *Limnology and Oceanography* 59, no. 6: 1910–1918. <https://doi.org/10.4319/lo.2014.59.6.1910>.

- Gray, P. C., A. E. Windle, J. Dale, et al. 2022. "Robust Ocean Color from Drones: Viewing Geometry, Sky Reflection Removal, Uncertainty Analysis, and a Survey of the Gulf Stream Front." *Limnology and Oceanography: Methods* 20, no. 10: 656–673. <https://doi.org/10.1002/lom3.10511>.
- Haigh, M. J. 1977. "The use of Erosion Pins in the Study of Slope Evolution." *British Geomorphological Research Group Technical Bulletin* 18: 31–49.
- Hansen, J. C. R., and M. A. Reidenbach. 2012. "Wave and Tidally Driven Flows in Eelgrass Beds and their Effect on Sediment Suspension." *Marine Ecology Progress Series* 448: 271–287. <https://doi.org/10.3354/meps09225>.
- Harrison, X. A., L. Donaldson, M. E. Correa-Cano, et al. 2018. "A Brief Introduction to Mixed Effects Modelling and Multi-Model Inference in Ecology." *PeerJ* 6: e4794. <https://doi.org/10.7717/peerj.4794>.
- Hothorn, T., F. Bretz, and P. Westfall. 2008. "Simultaneous Inference in General Parametric Models." *Biometrical Journal: Journal of Mathematical Methods in Biosciences* 50, no. 3: 346–363.
- Infantes, E., J. C. de Smit, E. Tamarit, and T. J. Bouma. 2021. "Making Realistic Wave Climates in Low-Cost Wave Mesocosms: A New Tool for Experimental Ecology and Biogeomorphology." *Limnology and Oceanography: Methods* 19: 317–330. <https://doi.org/10.1002/lom3.10425>.
- Infantes, E., S. Hoeks, M. P. Adams, T. van der Heide, M. M. van Katwijk, and T. J. Bouma. 2022. "Seagrass Roots Strongly Reduce Cliff Erosion Rates in Sandy Sediments." *Marine Ecology Progress Series* 700: 1–12. <https://doi.org/10.3354/meps14196>.
- Infantes, E., A. Orfila, G. Simarro, J. Terrados, M. Luhar, and H. Nepf. 2012. "Effect of a Seagrass (*Posidonia oceanica*) Meadow on Wave Propagation." *Marine Ecology Progress Series* 456: 63–72. <https://doi.org/10.3354/meps09754>.
- Jacobs, W., P. Le Hir, W. Van Kesteren, and P. Cann. 2011. "Erosion Threshold of Sand-Mud Mixtures." *Continental Shelf Research* 31, no. 10: S14–S25. <https://doi.org/10.1016/j.csr.2010.05.012>.
- Johansen, K., A. F. Dunne, Y.-H. Tu, S. Almashharawi, B. H. Jones, and M. F. McCabe. 2022. "Dye Tracing and Concentration Mapping in Coastal Waters Using Unmanned Aerial Vehicles." *Scientific Reports* 12, no. 1: 1141. <https://doi.org/10.1038/s41598-022-05189-9>.
- Kaufman, K. A., and S. S. Bell. 2022. "The Use of Imagery and GIS Techniques to Evaluate and Compare Seagrass Dynamics across Multiple Spatial and Temporal Scales." *Estuaries and Coasts* 45, no. 4: 1028–1044. <https://doi.org/10.1007/s12237-020-00773-6>.
- Kearney, S. P., S. J. Fonte, E. García, and S. M. Smukler. 2018. "Improving the Utility of Erosion Pins: Absolute Value of Pin Height Change as an Indicator of Relative Erosion." *Catena* 163: 427–432. <https://doi.org/10.1016/j.catena.2017.12.008>.
- Larson, R., A. Morang, and L. Gorman. 1997. "Monitoring the Coastal Environment; Part II: Sediment Sampling and Geotechnical Methods." *Journal of Coastal Research* 13, no. 2: 308–330.
- Lewis, C. J. E., and K. J. McGlathery. 2023. "A Novel Subsurface Sediment Plate Method for Quantifying Sediment Accumulation and Erosion in Seagrass Meadows." *Frontiers in Marine Science* 10: 1232619. <https://doi.org/10.3389/fmars.2023.1232619>.
- Marin-Diaz, B., C. Angelini, C. Pezoldt, K. Konchar, and A. H. Altieri. 2025. "Testing Biodegradable Interventions to Disrupt Plant-Animal Feedbacks and Promote Seagrass Establishment." *Restoration Ecology* 34: e70235. <https://doi.org/10.1111/rec.70235>.
- Marin-Diaz, B., T. J. Bouma, and E. Infantes. 2020. "Role of Eelgrass on Bed-Load Transport and Sediment Resuspension Under Oscillatory Flow." *Limnology and Oceanography* 65, no. 2: 426–436. <https://doi.org/10.1002/lno.11312>.
- McLeod, E., G. L. Chmura, S. Bouillon, et al. 2011. "A Blueprint for Blue Carbon: Toward an Improved Understanding of the Role of Vegetated Coastal Habitats in Sequestering CO<sub>2</sub>." *Frontiers in Ecology and the Environment* 9, no. 10: 552–560. <https://doi.org/10.1890/110004>.
- Murray, N. J., S. R. Phinn, M. DeWitt, et al. 2019. "The Global Distribution and Trajectory of Tidal Flats." *Nature* 565, no. 7738: 222–225. <https://doi.org/10.1038/s41586-018-0805-8>.
- Nepf, H. M. 2012. "Flow and Transport in Regions With Aquatic Vegetation." *Annual Review of Fluid Mechanics* 44, no. 1: 123–142. <https://doi.org/10.1146/annurev-fluid-120710-101048>.
- Nittrouer, C. A., and L. D. Wright. 1994. "Transport of Particles Across Continental Shelves." *Reviews of Geophysics* 32, no. 1: 85–113. <https://doi.org/10.1029/93RG02603>.
- Nolte, S., E. C. Koppenaal, P. Esselink, et al. 2013. "Measuring Sedimentation in Tidal Marshes: A Review on Methods and Their Applicability in Biogeomorphological Studies." *Journal of Coastal Conservation* 17, no. 3: 301–325. <https://doi.org/10.1007/s11852-013-0238-3>.
- Novo, E. M. M., J. D. Hansom, and P. J. Curran. 1989. "The Effect of Sediment Type on the Relationship Between Reflectance and Suspended Sediment Concentration." *International Journal of Remote Sensing* 10, no. 7: 1283–1289. <https://doi.org/10.1080/01431168908903967>.
- Ondiviela, B., G. García-Castrillo, M. Recio, A. Puente, and J. A. Juanes. 2015. "Cantabria." In Atlas de las praderas marinas de España, edited by J. M. Ruiz, J. E. Guillén, A. R. Segura, and M. M. Otero, 567–593. Instituto Español de Oceanografía / Instituto de Ecología Litoral / Unión Internacional para la Conservación de la Naturaleza (IEO/IEL/UICN).
- Ortiz, J. D., and A. A. Klompaker. 2015. "Turbidity Currents: Comparing Theory and Observation in the Lab." *Oceanography* 28, no. 3: 220–227. <https://doi.org/10.5670/oceanog.2015.73>.
- Pereda-Briones, L., E. Infantes, A. Orfila, F. Tomas, and J. Terrados. 2018. "Dispersal of Seagrass Propagules: Interaction Between Hydrodynamics and Substratum Type." *Marine Ecology Progress Series* 593: 47–59. <https://doi.org/10.3354/meps12518>.

- Pope, S. B. 2000. *Turbulent Flows*. Cambridge University Press.
- Potouroglou, M., J. C. Bull, K. W. Krauss, et al. 2017. "Measuring the Role of Seagrasses in Regulating Sediment Surface Elevation." *Scientific Reports* 7, no. 1: 11917. <https://doi.org/10.1038/s41598-017-12354-y>.
- R Core Team. 2025. R: A Language and Environment for Statistical Computing. R Foundation for Statistical Computing. <https://www.r-project.org/>.
- Russell, B. T., K. A. Cressman, J. P. Schmit, S. Shull, J. M. Rybczyk, and D. L. Frost. 2022. "How Should Surface Elevation Table Data be Analyzed? A Comparison of Several Commonly Used Analysis Methods and One Newly Proposed Approach." *Environmental and Ecological Statistics* 29, no. 2: 359–391. <https://doi.org/10.1007/s10651-021-00524-1>.
- Sclavo, M., A. Benetazzo, S. Carniel, A. Bergamasco, F. M. Falcieri, and D. Bonaldo. 2013. "Wave-Current Interaction Effect on Sediment Dispersal in a Shallow Semi-Enclosed Basin." *Journal of Coastal Research* 165: 1587–1592. <https://doi.org/10.2112/SI65-268.1>.
- Soulsby, R. 1997. *Dynamics of Marine Sands: A Manual for Practical Applications*. London: Thomas Telford. <https://doi.org/10.1680/doms.25844>.
- Soulsby, R. L., and J. S. Damgaard. 2005. "Bedload Sediment Transport in Coastal Waters." *Coastal Engineering* 52, no. 8: 673–689. <https://doi.org/10.1016/j.coastaleng.2005.04.003>.
- Soulsby, R. L., L. Hamm, G. Klopman, D. Myrhaug, R. R. Simons, and G. P. Thomas. 1993. "Wave-Current Interaction Within and Outside the Bottom Boundary Layer." *Coastal Engineering* 21, no. 1–3: 41–69. [https://doi.org/10.1016/0378-3839\(93\)90045-A](https://doi.org/10.1016/0378-3839(93)90045-A).
- Stokes, D. J., T. R. Healy, and P. J. Cooke. 2010. "Expansion Dynamics of Monospecific, Temperate Mangroves and Sedimentation in Two Embayments of a Barrier-Enclosed Lagoon, Tauranga Harbour, New Zealand." *Journal of Coastal Research* 26, no. 1: 113–122. <https://doi.org/10.2112/08-1043.1>.
- Swales, A., and C. E. Lovelock. 2020. "Comparison of Sediment-Plate Methods to Measure Accretion Rates in an Estuarine Mangrove Forest (New Zealand)." *Estuarine, Coastal and Shelf Science* 236: 106642. <https://doi.org/10.1016/j.ecss.2020.106642>.
- Temmerman, S., P. Meire, T. J. Bouma, P. M. J. Herman, T. Ysebaert, and H. J. De Vriend. 2013. "Ecosystem-Based Coastal Defence in the Face of Global Change." *Nature* 504, no. 7478: 79–83. <https://doi.org/10.1038/nature12859>.
- Temmink, R. J., M. J. Christianen, G. S. Fivash, et al. 2020. "Mimicry of Emergent Traits Amplifies Coastal Restoration Success." *Nature Communications* 11, no. 1: 3668. <https://doi.org/10.1038/s41467-020-17438-4>.
- Tennekes, H., and J. L. Lumley. 1972. *A First Course in Turbulence*. MIT Press.
- Thomas, S., and P. V. Ridd. 2004. "Review of Methods to Measure Short Time Scale Sediment Accumulation." *Marine Geology* 207, no. 1–4: 95–114. <https://doi.org/10.1016/j.margeo.2004.03.011>.
- Thomas, S., P. V. Ridd, and P. J. Smith. 2002. "New Instrumentation for Sediment Dynamics Studies." *Marine Technology Society Journal* 36, no. 1: 55–58. <https://doi.org/10.4031/002533202787914278>.
- Van Duin, W. E., K. S. Dijkema, and J. Zegers. 1997. "Veranderingen in bodemhoogte (opslibbing, erosie en inklink) in de Peazemerlannen." <https://sciwheel.com/work/bibliography/18194793>.
- van Wijnen, H. J., and J. P. Bakker. 2001. "Long-Term Surface Elevation Change in Salt Marshes: A Prediction of Marsh Response to Future Sea-Level Rise." *Estuarine, Coastal and Shelf Science* 52, no. 3: 381–390. <https://doi.org/10.1006/ecss.2000.0744>.
- Veettil, B. K., R. D. Ward, M. D. A. C. Lima, M. Stankovic, P. N. Hoai, and N. X. Quang. 2020. "Opportunities for Seagrass Research Derived From Remote Sensing: A Review of Current Methods." *Ecological Indicators* 117: 106560. <https://doi.org/10.1016/j.ecolind.2020.106560>.
- Wang, D., and J. Yuan. 2018. "Bottom-Slope-Induced Net Sediment Transport Rate under Oscillatory Flows in the Rippled-Bed Regime." *Journal of Geophysical Research: Oceans* 123, no. 10: 7308–7331. <https://doi.org/10.1029/2018JC013810>.
- Wiberg, P., and J. D. Smith. 1983. "A Comparison of Field Data and Theoretical Models for Wave-Current Interactions at the Bed on the Continental Shelf." *Continental Shelf Research* 2, no. 2–3: 147–162. [https://doi.org/10.1016/0278-4343\(83\)90013-4](https://doi.org/10.1016/0278-4343(83)90013-4).
- Widdows, J., N. D. Pope, and M. D. Brinsley. 2008. "Effect of *Spartina Anglica* Stems on Near-Bed Hydrodynamics, Sediment Erodability and Morphological Changes on an Intertidal Mudflat." *Marine Ecology Progress Series* 362: 45–57. <https://doi.org/10.3354/meps07448>.
- Woodroffe, C. D., and C. V. Murray-Wallace. 2012. "Sea-Level Rise and Coastal Change: The Past as a Guide to the Future." *Quaternary Science Reviews* 54: 4–11. <https://doi.org/10.1016/j.quascirev.2012.05.009>.
- Wright, L. D., and B. G. Thom. 2023. "Coastal Morphodynamics and Climate Change: A Review of Recent Advances." *Journal of Marine Science and Engineering* 11, no. 10: 1997. <https://doi.org/10.3390/jmse11101997>.
- Yang, J. Q., and H. M. Nepf. 2019. "Impact of Vegetation on Bed Load Transport Rate and Bedform Characteristics." *Water Resources Research* 55, no. 7: 6109–6124. <https://doi.org/10.1029/2018WR024404>.

### Supporting Information

Additional Supporting Information may be found in the online version of this article.

Submitted 01 December 2025

Revised 27 May 2026

Accepted 03 June 2026